

# **Figure Control of Lightweight Optical Structures**

NCC-1-385

John A. Main, Principal Investigator  
Haiping Song, Postdoctoral Research Associate  
Department of Mechanical Engineering  
University of Kentucky  
Lexington, KY 40506-0503

## **Abstract**

The goal of this paper is to demonstrate the use of fuzzy logic controllers in modifying the figure of a piezoceramic bimorph mirror. Non-contact electron actuation technology is used to actively control a bimorph mirror comprised two PZT-5H wafers by varying the electron flux and electron voltages. Due to electron blooming generated by the electron flux, it is difficult to develop an accurate control model for the bimorph mirror through theoretical analysis alone. The non-contact shape control system with electron flux blooming can be approximately described with a heuristic model based on experimental data. Two fuzzy logic feedback controllers are developed to control the shape of the bimorph mirror according to heuristic fuzzy inference rules generated from previous experimental results. Validation of the proposed fuzzy logic controllers is also discussed.

Keywords: Bimorph mirror, Electron gun, Fuzzy logic controller

## **1. Introduction**

Piezoelectric actuators have been used for shape control since the earliest development of adaptive mirrors. In 1974, a monolithic piezoelectric mirror was designed using piezoelectric ceramic stacks to induce a deformation on a the mirror surface<sup>[1]</sup>. Steinhaus et. al<sup>[2]</sup> investigated a piezoelectric flexible mirror with multiple electrodes to control numerous discrete areas. This consisted of a bonded layer of piezoceramic on the back of a thin glass mirror; a continuous electrode was located at the interface and an array of twelve electrodes was distributed on the back of mirror. Microelectronic techniques were used to build a segmented bimorph deformable mirror using low-voltage bending PZT bimorph wafers<sup>[3]</sup>. Another bimorph design used PZT with a continuously grounded electrode between the layers deposited on either side of the bimorph<sup>[4]</sup>. Other composite deformable mirrors <sup>[5,6]</sup> were developed by embedding multiple piezoelectric actuator patches in the laminates during fabrication. These implementations require a complex power supply with multiple channels and a corresponding controller to control multiple electrodes dynamically. In addition, the size and placement of actuator patches could not be adjusted after the mirror was manufactured.

To simplify the mirror structure and control system, a non-contact technique for deformable mirror control using an electron gun control has recently been proposed<sup>[7]</sup>. The authors have developed a bimorph mirror that consists of two PZT-5H wafers 50.8 mm in diameter, 1mm thick, and cemented together with RTV-11 glue. One surface is polished and has deposited on it a reflective aluminum surface. Of course, the obvious advantages of this system is that the mirror structure is much less complex than

adaptive mirrors using conventional actuators and the addressable areas in the mirror are not defined by the system hardware.

Hubbard <sup>[8]</sup> initially considered use of electron gun actuation for control of deformable mirrors. In this case the mirror was constructed from a PVDF bimorph. Main and Nelson <sup>[9,10]</sup> demonstrated that the strain in piezoelectric materials could be controlled through a combination of applied electron beams and control voltage to the opposite surface. This approach was similarly used to control the shape of membrane mirrors <sup>[11]</sup>. An improved electron gun actuation method was proposed by placement of a screen collector near to the PZT surface<sup>[7]</sup>. Results indicated that the method is capable of producing positive and negative deformation of a mirror in a very short time. Since the electron accumulation on PZT material may remain relatively static even after the removal of the electron beam, the electron gun control method has the ability to actuate distributed points simultaneously similar to multiple electrodes attached to the mirror.

Significant advantages of non-contact electron gun control include a simplified mirror structure as well as high spatial and temporal resolution in the excitation areas. Nevertheless, the collision dynamics of the electron with the surface of a PZT material is complex due to the nature of the energy transfer, secondary electron yield and absorbed electron blooming<sup>[12]</sup>. Therefore, the deflection response of a bimorph mirror using electron flux excitation cannot be expressed precisely even though an analysis tool (for example, ANSYS<sup>®</sup>), can be used to simulate the electromechanical coupling behavior of the PZT bimorph. The control method discussed in this paper is an

uncertain system, which can be approximately described with the heuristic variables according to previous experimental results.

Fuzzy logic control (FLC) is advantageous for nonlinear or uncertain systems<sup>[13]</sup>. An obvious advantage of FLC techniques is the synthesis of human knowledge and expertise in dealing with uncertainties in the control phase. Fuzzy logic control usually decomposes a complex system into several local systems according to the expert's understanding of the subsystem and uses a simple control law to emulate the expert's control strategy in performing certain control tasks. Fuzzy systems provide a general methodology for representing the complexity of real world problems. FLC algorithms will be applied herein to correct the shape of a bimorph mirror with a non-contact closed loop control system. The excitation of electron flux and two controllable voltages on the surface of the mirror and on the screen collector, respectively, will be used as actuation inputs. A wavefront sensor will be utilized to measure the mirror profile to provide shape feedback.

## **2. Experimental setup and feedback control system**

### **2.1 Experimental setup**

The experimental setup, as shown in Figure 1, consists of a bimorph mirror, an electron gun system, two voltage control amplifiers, a wavefront sensing light measurement system, a dSPACE controller system and a vacuum chamber. The bimorph mirror is a composite layer structure consisting of a PZT bimorph mounted on a self-centering jaw clamp with three constraint points. The electron gun system includes an electron gun, a power supply and a localizer. The electron gun is a Kimball Physics

EFG-7. The electron gun power supply is used to adjust electron beam energy, focus the beam, and switch the beam on or off, while the localizer is used to control shooting points on the mirror. The voltage control amplifiers are used to supply the backpressure voltage on the surface of the mirror and the collector. The dSPACE controller system consists of a PC with an interface unit consisting of multi-channel D/A and digital I/O ports.

Since the electron gun can only be operated in a vacuum environment (approximately  $10^{-5}$  Torr minimum), the mirror, electron gun and screen electron collector are mounted in the chamber. The wavefront sensor (Wavefront Sciences CLAS-2D) measures the modal deformation through a window in the chamber; the corresponding deformation information of the mirror is fed into the dSPACE control computer. The dSPACE controller calculates the magnitudes of controllable variables applied to relevant voltage amplifiers and to the electron gun system.

The wavefront system is a Shack-Hartmann sensor in which the Zernike polynomials (shown in Equation 1) are implemented using modal reconstruction to recreate the phase  $\phi(x, y)$ . The order of the polynomial fit that describes the surface will directly affect both the processing time and the visibility of higher order terms. For acquiring a phase of the mirror in appropriate computing time for the closed loop control, a fourth order polynomial is used, as it is generally an adequate option for most tests <sup>[14]</sup>. The phase  $\phi(x, y)$  is given by

$$\begin{aligned} \phi(x, y) = & a_{00} + a_{10}Z_{10}(x, y) + a_{11}Z_{11}(x, y) + a_{20}Z_{20}(x, y) + a_{21}Z_{21}(x, y) \\ & + a_{22}Z_{22}(x, y) + \cdots + a_{nk}Z_{nk}(x, y) + \cdots \end{aligned} \quad (1)$$

where  $Z_{nk}(x, y)$  is the  $k^{\text{th}}$  Zernike polynomial of  $n$ th order and  $a_{nk}$  refers to the coefficient of  $Z_{nk}(x, y)$ .

In the dSPACE control computer, a Matlab simulink program was converted into real-time code that is utilized to operate dSPACE's digital I/O board and A/D-D/A board to control the electron gun parameters. Moreover, the Matlab-dSPACE interface has the ability to control an experiment via a Matlab script.

## 2.2 Selection of input and output variables

The controllers explored in the current effort are used to modify the shape of a bimorph mirror to a desired profile. The wavefront sensor is used to measure the mirror profile and feedback this to the controller. Thus, the error between measured profile and desired profile can be defined as input variables.

The goal of shape control process can be represented as

$$\mathbf{e}_w(k) = \mathbf{w}(k) - \mathbf{w}_d \Rightarrow 0 \quad (2)$$

where  $\mathbf{w}_d$  is a desired deflection matrix of a bimorph mirror, and  $\mathbf{w}(k)$  and  $\mathbf{e}_w(k)$  represent a measured deflection matrix and corresponding error matrix, respectively.

Since the deflection of the mirror's profile measured by the WFS is always positive, a transformation of the error matrix can be performed through the computation of average error on the mirror such as

$$\bar{\mathbf{e}}_w(k) = \mathbf{e}_w(k) - \text{avg}(\mathbf{e}_w(k)) \quad (3)$$

Then, the maximum and minimum values in  $\bar{\mathbf{e}}_w(k)$  and their coordinates can be obtained by the following formulae.

$$w_c^1(k) = \max(\hat{e}_w(k)) \quad w_c^2(k) = \min(\hat{e}_w(k)) \quad (4)$$

Obviously,  $w_c^1(k)$  is positive and  $w_c^2(k)$  is negative. Their corresponding positions on the profile of the wavefront sensor can be conveniently derived from the wavefront phase matrix. Therefore, the maximum and minimum errors of deflections on the mirror can be defined as points of excitation for an electron flux and thus are also input variables for the controller. Note that actuating points on the mirror are variable when using the noncontact electron gun control method.

Due to the influence of boundary constraints on the mirror, different areas on the mirror actuated with the same values of input control variables can produce different mirror deformations. A finite element model for this kind of bimorph mirror has been constructed in ANSYS 5.7 to calculate the deformation of the mirror. The bimorph mirror structure has been modeled by SOLID5 elements with a 6 node 3-D coupled-field brick element with piezoelectric and structural field capability. The back of the mirror model is excited at 100 volts at a point 1mm in diameter, with the corresponding ground simultaneously connected to the mirror surface. It is assumed that the polarization in the PZT-5H sheet is uniform and perpendicular to the surface of the mirror and anti-parallel in successive layers. The piezoelectric and mechanical properties of PZT-5H are summarized in Table 1, in which  $C_{ij}$  are the elastic stiffness constants,  $e_{ij}$  the piezoelectric constants and  $\epsilon_{ij}$  the dielectric constants. It is noted that  $C_{66} = \frac{1}{2}(C_{11} - C_{12})$ .

Exciting nine different points on the back of mirror, as shown in Figure 2, makes use of the finite element model to analysis out-of-plane deformations of the bimorph mirror according to the no blooming assumption of the electrode in a PZT-5H sheet. An

analytical result of the bimorph mirror is shown in Figure 3 and the maximum deflections on nine different spots are shown in Figure 4. Results illustrate that the more distant the excitation spot is from the constraint points, the larger the deformation of the mirror at the same input voltage. Thus, the position of the actuating point can be considered as an input variable.

Output variables should include the position of actuation points, electron gun operating parameters, and control voltages. The position of the actuation points can be directly delivered to the localization system of the electron gun. Though there are many variables used to control the electron gun (for example, energy level, focusing area, source and grid voltages, etc.), only electron gun energy ( $V_e$ ) was used as a control variable to simplify the controller output as well as following the results of previous experiments. Other parameters of the electron gun can be set to invariants or functions of energy; for the experiment discussed herein, the source voltage is equal to 1.4 V, focus/energy is 0.65 on the Kimball Physics EFG-7 in order to produce a minimum beam point on the object, and the grid voltage ( $V_g$ ) is used to turn on or off the electron beam current. As the grid voltage is increased, the cathode emission is suppressed and eventually completely cut off. The grid voltage is expressed by an empirical formula obtained by measuring the emission current while adjusting grid voltage.

$$V_g = \begin{cases} 0.062 \times (V_e - 500) + 15 & \text{if } V_e > 400 \\ 8.80 & \text{if } V_e \leq 400 \end{cases} \quad (5)$$

The shooting time of the electron flux ( $T_e$ ) is also an important adjustable parameter that can be determined by altering grid voltage.

In summary, the control variables in this system are the backpressure voltage ( $V_b$ ) on the mirror surface, the collector voltage ( $V_c$ ) on the screen collector, the energy voltage ( $V_e$ ) of the electron gun as well as the shooting time ( $T_e$ ) of the electron flux. Based on these definitions of input and output variables, Figure 5 shows a block diagram of the discrete feedback control system for the control of a bimorph mirror, in which two points are excited in each control loop.

### **3. Fuzzy logic control with discrete feedback**

Fuzzy logic control utilizes knowledge of process control based on human perspective and experience. Thus, the designer is required to have sufficient knowledge of how the mechanism of the system functionally operates, plus a good idea of how the control system should behave. The actuating mechanism of the non-contact control discussed herein is inherently more complicated than a conventional actuator. The actuator is dependent on the electron flux that is induced by a provided energy voltage, source voltage, focus voltage, and the shooting time. In addition, both backpressure and collector voltages are important parameters to in deformation characteristics. Therefore, this can be classified as an uncertain system that cannot be described with an approximated mathematical relationship. However, this system can be represented with some simple heuristic expressions. Thus, we use a fuzzy logic scheme for shape control of the bimorph mirror system.

In designing a fuzzy logic controller, one must be able to identify control variables (i.e., heuristic parameters) in order to describe inputs and outputs of the fuzzy system. The heuristic quantification is used to create a set of rules that contain the control

process rules. In this section, fuzzy inference algorithms using single-input/multi-output (SIMO) and multi-input/multi-output (MIMO) schemes for each excitation point on the surface of PZT-5H sheet are developed in order to control the mirror shape effectively. The fuzzy control system is shown in Figure 6.

### 3.1 SIMO fuzzy logic control

One can see from Figure 5 that there are two excitation points in every control loop. At first, we consider the deflection error on each excitation point as a single input variable of the non-contact-actuating controller. In this control procedure, the backpressure voltage ( $V_b$ ), the collector voltage ( $V_c$ ), the electron gun energy voltage ( $V_e$ ) and its shooting time ( $T_e$ ) are defined as the output variables. For construction of a simple fuzzy inference model for a non-contact-actuating controller, we consider maximum or minimum deflection error ( $w_c^1(k), w_c^2(k)$ ) as three heuristic items; i.e., {WN, WZ, WP}, where WN is a negative deflection error, WZ is a zero deflection error and WP is a positive deflection error. Their membership functions, shown in Figure 7, were defined as Z-, triangular- and S-shaped curves, respectively.

Based on previous experimental results<sup>[7]</sup>, four output control variables can be determined from their rational heuristic variables. Three heuristic terms, i.e. {BN, BZ, BP}, are used to define the backpressure voltage ( $V_b(k)$ ). These items consist of Z-shaped, triangular and S-shaped membership functions in which BN, BZ and BP express negative, zero and positive backpressure voltages respectively. Additionally, three other output variables are always defined in the positive numerical range. We define the screen collector voltage ( $V_c(k)$ ), the electron flux energy ( $V_e(k)$ ) and the

electron flux shooting time ( $T_e(k)$ ) as fuzzy heuristic items {CS, CL}, {ES, EM, EL} and {TS, TL}, where, 'C', 'E' and 'T' represent the collector voltage, the electron energy and the actuation time, respectively. Here, 'S', 'M' and 'L' represent small, middle and large values, respectively. Their membership functions shown in Figure 8 are summarized from a number of previous experimental results.

The fuzzy logic rule base is usually in the form of IF-THEN rules that are derived from experimental results on how to control the plant in order to effectively link the input and output variables. The establishment of these rule bases depends heavily on the designer's experience, knowledge about the plant, analysis and design skill, etc. For the shape control of the bimorph mirror, two general rules are composed as follows:

$$\begin{aligned} &\text{IF error is positive, THEN actuating force is negative} \\ &\text{IF error is negative, THEN actuating force is positive} \end{aligned} \quad (6)$$

This means that a negative actuating force is used to deform the mirror to decrease the error of deflection on the mirror when the error is positive. The reverse is also true. In the non-contact shape control system, the actuating force is roughly decided by four controllable parameters;  $V_b, V_c, V_e$  and  $T_e$ . Hence, the fuzzy logic controller based on rule base in Equation 6 should be a single-input and multi-output system and a fuzzy inference mechanism must be constructed to obtain the four output variables from single input variable. Three rules applied to the shape control of the bimorph mirror are constructed as follows:

Rule1: IF  $w_c(k)$  is 'WN'

THEN  $V_b(k)$  is 'BP' and  $V_c(k)$  is 'CS' and  $V_e(k)$  is 'EL' and  $T_e(k)$  is 'TS'

Rule2: IF  $w_c(k)$  is 'WP'

THEN  $V_b(k)$  is 'BN' and  $V_c(k)$  is 'CL' and  $V_e(k)$  is 'EM' and  $T_e(k)$  is 'TL' (7)

Rule3: IF  $w_c(k)$  is 'WZ'

THEN  $V_b(k)$  is 'BZ' and  $V_c(k)$  is 'CS' and  $V_e(k)$  is 'ES' and  $T_e(k)$  is 'TS'

The inference mechanism is divided into two subsections. The first operation is the determination of the applicability of each rule according to the fuzzification of  $w_c(k)$ , represented with a membership function shown in Figure 7. Since the input value is very large in a positive direction and very small in a negative direction, the value of the input membership function might be defined as 1. The second step in the inference section is to obtain the output variables from the rules. Once the condition of deflection error has been determined, the output variables can be calculated by the inverse computation of their corresponding membership functions according to the fuzzy rules. For example, if  $w_c(k)$  is a negative value ( $0 < w_c(k) < -1$ ), its membership function value ( $\mu_w(k)$ ) can be computed with a Z-shaped curve membership function and the output variable ( $V_b(k)$ ) is positive (BP) as given from rule1. It is assumed that

$$\mu_b(k) = \mu_w(k) \quad (8)$$

Then, a defuzzification process can be used to obtain crisp control output ( $V_b(k)$ ). That is accomplished through the computation of an inverse S-shaped membership function. If the fuzzy range of backpressure voltage is defined as  $[V_0, V_1]$ ,  $V_b(k)$  can be acquired by

$$V_b(k) = \begin{cases} V_1 - (V_1 - V_0) \cdot \sqrt{\frac{(1 - \mu_b(k))}{2}} & \text{if } \mu_b(k) \geq 0.5 \\ V_1 + (V_1 - V_0) \cdot \sqrt{\frac{\mu_b(k)}{2}} & \text{if } \mu_b(k) < 0.5 \end{cases} \quad (9)$$

The crisp values of other control variables can be acquired in the same way by considering the inverse function of their corresponding membership functions. The main purpose of defuzzification is to convert the result of fuzzy inference into a crisp result for the implementation of the control process.

### 3.2 MIMO fuzzy logic control

Analytical results from finite element analyses represent that deformations of the mirror actuated with the same controllable variables are different for different excitation points. The maximum deflections on the mirror also depend on the distance between the excitation point and constraint points. It is obvious that a greater deformation is achieved when the excitation point is further from the constraint points. Thus, a MIMO fuzzy logic controller for the system can be established by taking into consideration the deflection error and position of the excitation point as two input variables, and four adjustable parameters ( $V_b$ ,  $V_c$ ,  $V_e$  and  $T_e$ ) as four output variables. Five triangular membership functions for the deflection heuristic terms are given in Figure 9, {NL,NS,Z,PS,PL}. The fuzzy expression of the excitation point position ( $D_c$ ) is comprised of three heuristic terms, {DS,DM,DL}, and is shown in Figure 9.  $D_c$  is a minimum distance expressed by

$$D_c = \min(D_1, D_2, D_3) \quad (10)$$

where  $D_1$ ,  $D_2$  and  $D_3$  are the distance values from the excitation point to the three constraint points.

For the four output variables, membership functions using triangular functions are represented in Figures 10 and 11 in terms of previous experimental and analytical

results, where adjustable voltages  $V_b$  and  $V_c$  are described by eleven and ten heuristic terms, respectively, and the electron flux parameters  $V_e$  and  $T_e$  are defined by ten and eight heuristic terms, respectively. Accordingly, this MIMO fuzzy model for the shape control of the bimorph mirror can be expressed by a Mamdani fuzzy model<sup>[13]</sup>. The rule base of this fuzzy model shown in Table 2 consists of 15 rules for each output variable, adopted from all possible combinations of the antecedent terms.

To obtain sensible output, the defuzzification of the control variables has to take into account all of the recommendations from the inference mechanism. There are many different methods of combining the fuzzy sets to produce a crisp control output, the center of gravity technique being one of the more popular. This method is used with the Mamdani inference to provide interpolation between the consequences in proportion to the individual consequent sets. The fuzzy sets from the consequence of each rule are combined through the aggregate operator and the resulting fuzzy set is defuzzified to yield the output of the system. This method computes the crisp control output variable based on the area under the fuzzy sets by

$$V = \frac{\sum_{i=1}^r A_i f_i}{\sum_{i=1}^r A_i} \quad (11)$$

where  $A_i$  is the area under the membership function  $\mu_i$ ,  $f_i$  is a center of the membership function of the consequent of rule  $i$ ,  $r$  is the number of rules and  $V$  is a crisp output value. Note that  $\mu_i$  is 0.05 when  $w_c \geq 8\mu m$  or  $w_c \leq -8\mu m$  in order to obtain an appropriate output by avoiding  $A_i = 0$ .

#### 4. Experimental results and discussion

The aim of bimorph mirror shape control is to reduce the error of the bimorph mirror shape between the measured and desired shape by adjusting the out-of-plane deformations of the mirror with non-contact electron gun excitation through the presented control method, which is either a feedback control with SIMO or MIMO fuzzy logic control according to the observations from the wavefront sensor. The controlling goal can be defined as

$$\text{Min} J(k) = w_c^1(k) - w_c^2(k) \quad (11)$$

where  $J(k)$  is a control aim value and  $k$  expresses the  $k$ th discrete control loop.

The excitation points of the electron gun can be distributed to any possible position on the back of the mirror. To obtain the excitation points, a map is created from the measurement profile of the mirror to the real mirror geometry. Using Equations (3) and (4), we can determine two actuation points directly from the maximum and minimum error displacement points on the mirror in each control loop. However, these points could possibly be on the edge of a profile. As the shooting points of the electron gun are derived directly from the wavefront profile, these points might also be on the edge of the mirror structure that could be difficult for the electron flux to properly target. To avoid this problem, the location of the excitation points are determined by calculating the weighted average of the region nearest to the position of the maximum or minimum deflection with a 0.8 threshold value of the corresponding peak value.

Based on the assumption that the desired shape of the mirror is nearly flat, two experiments have been implemented by using the two types of FLC controllers proposed in section 3, respectively. Figure 12a and 12b show the response of absolute

maximum deflection and max-min deflections on the mirror, respectively, with respect for the SIMO fuzzy controller. The absolute maximum deflection can be reduced from 24.27  $\mu\text{m}$  to 10.12  $\mu\text{m}$  in sixteen control loops. Figure 13a and 13b show the deflection response of the absolute maximum and max-min errors, respectively, using the MIMO fuzzy controller. The absolute maximum deflection has been decreased from 19.85  $\mu\text{m}$  to 6.91  $\mu\text{m}$  in nine control loops. Though both control methods can effectively reduce the deformation of the bimorph mirror in several control steps, the MIMO fuzzy controller has a more efficient solution than the SIMO fuzzy controller.

Figures 14a and 14b show the initial and controlled profiles of the bimorph mirror with the SIMO fuzzy controller while figures 15a and 15b show the initial and controlled profiles of the mirror with MIMO fuzzy controller, respectively. The experimental results illustrate that the fuzzy control methods are more effective for shape control, but these control methods cannot produce a desired shape of the mirror since the collision mechanism of electrons on a PZT-5H sheet is complex. Actually, the shape of the mirror is adjusted by controlling the electric field across its thickness. The net electric field is the result of the potential on the PZT-5H wafer and the potential of the mirror/electrode controlled by a power amplifier. The accumulation amount and distribution position of electrons on the PZT-5H wafer are important factors for inducing deformation on the mirror. They are not only determined by control voltages ( $V_b, V_c$ ), but also by accumulated electrons on the back of the mirror. Future work includes the development of a more robust intelligent control method that is able to correct the bimorph mirror into any desired shape.

## 5. Conclusions

The purpose of this research is to form and develop a simple closed-loop control system with fuzzy logic for non-contact electron gun control of a bimorph mirror. A SIMO and a MIMO fuzzy inference mechanism based on previous experimental results was derived to construct two fuzzy logic controllers for non-contact shape control of the mirror. A wavefront sensor was used as the feedback device. Both the SIMO and MIMO models demonstrated the ability to correct the mirror deformation. Due to the complexity of the excitation process, the closed loop control between the measured shape and corrective electron gun actuation with fuzzy logic is still not a perfect solution, but experimental results show that the fuzzy logic control methods are effective in correcting the shape of the mirror to a desired shape, though not with total accuracy. Further work is necessary to develop an adaptive intelligent control method so that the control model can be trained in the control process.

## References

1. Feinleib, J. Lipson, G. and Cone P. F. "Monolithic piezoelectric mirror for wavefront correction", Applied Physics Letters 1974 Vol.25, No.5 pp311-313
2. Steinhaus, E, Lipson, S.G, "Bimorph piezoelectric flexible mirror" Journal of the Optical Society of America, 1979, Vol.69 pp. 478-481
3. Forbes, F., Roddier, F., Poczulp, G., Pinches, C., Sweeny, G. and Dueck, R., "Segmented bimorph deformable mirror", Journal of Physics E: Scientific Instruments, 1989, Vol.22 pp402-405

4. Susini, J., D. Labergerie and L. Zhang. "Compact active/adaptive X-ray mirror:bimorph piezoelectric flexible mirror." *Review of Scientific Instruments* (1995), Vol.66 pp2229-2231.
5. Kuo, CP, Wada BK. Composite deformable mirror. *Active Telescope Systems* 1989;Vol. 1114, pp 495-505
6. Paradies, R., Hertwig, M. "Shape control of adaptive composite reflectors", *Composites: Part B*. 1999, Vol.30 pp65-78
7. Song, H and Main, J. A, "Non-contact closed loop control system of optic deformable mirrors" in preparation.
8. Hubbard, J. "Active mirror assembly" United States Patent, #5,159,498 October,1992
9. Main, J.A, Nelson, G.C, "Smart material control system and related method", United States Patent#6,188,160 February, 2001.
10. Nelson, G.C., Main, J.A., "Non-contact Electron Gun Strain Control of Piezoceramics" *AIAA Journal*, 2001, Vol. 39, No. 9, pp.1808-1813.
11. Martin, J., Main, J. A, and Nelson, G. C, "Shape Control of Deployable Membrane Mirrors," *Proceedings of the ASME International Mechanical Engineering Congress and Exposition, Adaptive Structures and Material Systems*, Anaheim California, November 15-20, 1998, AD-Vol. 57, pp. 217-223.
12. Ganachaud, J.P, Mokrani, A. "Theoretical Study of the Secondary Electron Emission of Insulating Target" *Surface Science* 1995, Vol. 334, No. 1-3, pp329-341.
13. Nguyen, H.T. and Sugeno, M. "Fuzzy Systems Modeling and Control", Kluwer Academic Publishers, 1998
14. Neal, D.R. Armstrong, D.J. and Turner, W.T. "Wavefront sensors for control and process monitoring in optics manufacture" *SPIE* 2993(29) 1997

Table 1. Material Properties of PZT-5H

Properties	Unit	Value
$C_{ij}$	$10^{10}\text{Nm}^{-2}$	$C_{11}=C_{22}=12.72, C_{12}=8.02,$ $C_{13}=C_{23}=8.47, C_{33}=11.74,$ $C_{44}=C_{55}=2.30$
$e_{ij}$	$\text{Cm}^{-2}$	$e_{31}=e_{32}=-6.62, e_{33}=23.24,$ $e_{15}=e_{14}=17.03$
$\varepsilon_{ij}$	$10^{-9}\text{Fm}^{-1}$	$\varepsilon_{11}=\varepsilon_{22}=27.71, \varepsilon_{33}=30.10$

Table 2. Rule bases of MIMO fuzzy model

$V_b$		$W_c$				
		NL	NS	Z	PS	PL
$D_c$	DS	PLL	PM	Z	NM	NLL
	DM	PLS	PSL	Z	NSL	NLS
	DL	PM	PSS	Z	NSS	NM

$V_c$		$W_c$				
		NL	NS	Z	PS	PL
$D_c$	DS	SS	SM	SS	LM	LL
	DM	SMS	SML	SS	LMS	LML
	DL	SM	SL	SS	LS	LM

$V_e$		$W_c$				
		NL	NS	Z	PS	PL
$D_c$	DS	LL	LM	SS	SM	SL
	DM	LML	LMS	SS	SMS	SML
	DL	LM	LS	SS	SS	SM

$T_e$		$W_c$				
		NL	NS	Z	PS	PL
$D_c$	DS	SL	SML	SS	LML	LL
	DM	SML	SMS	SS	LMS	LML
	DL	SMS	SS	SS	LS	LMS

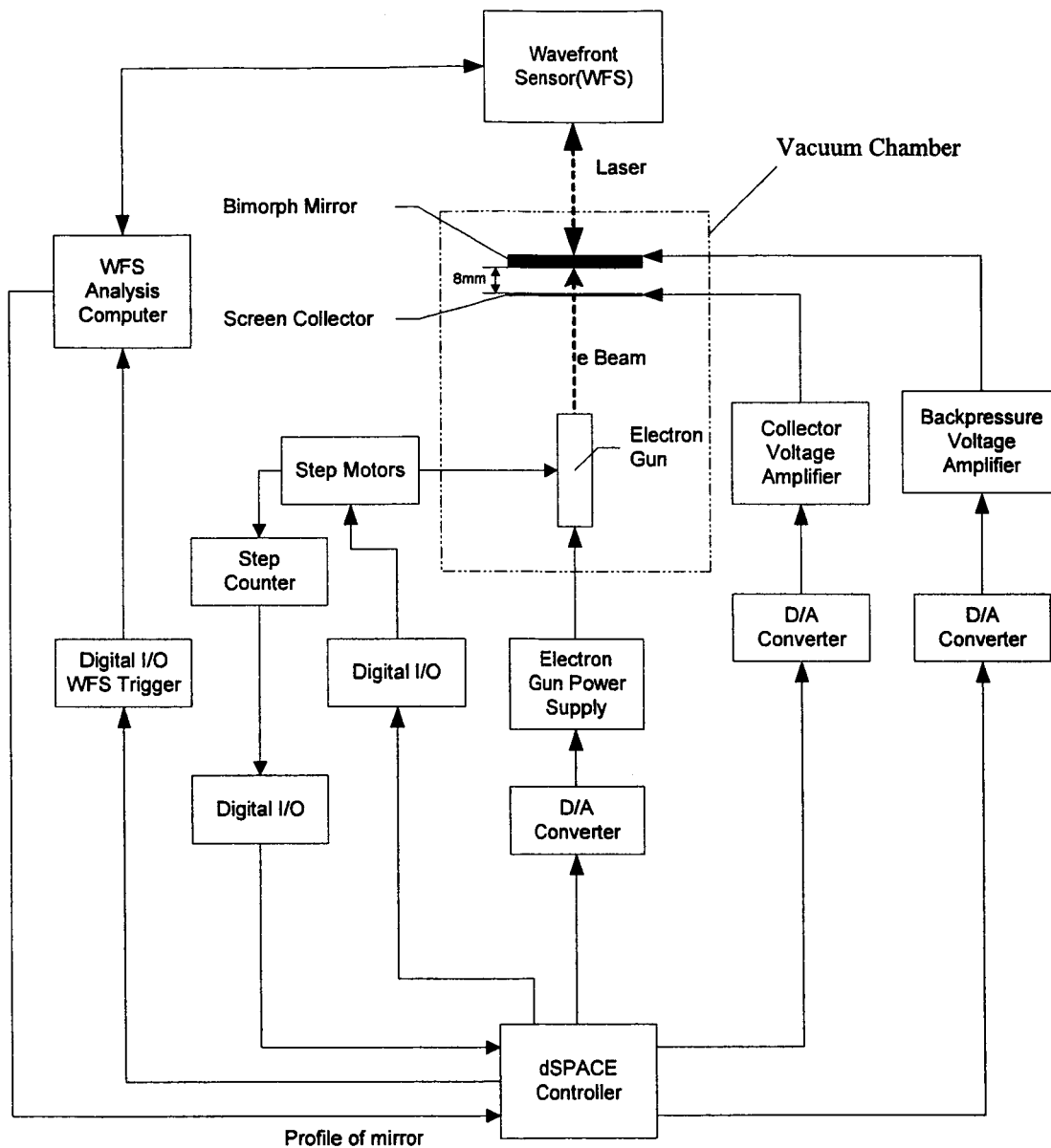


Figure 1. The experimental setup

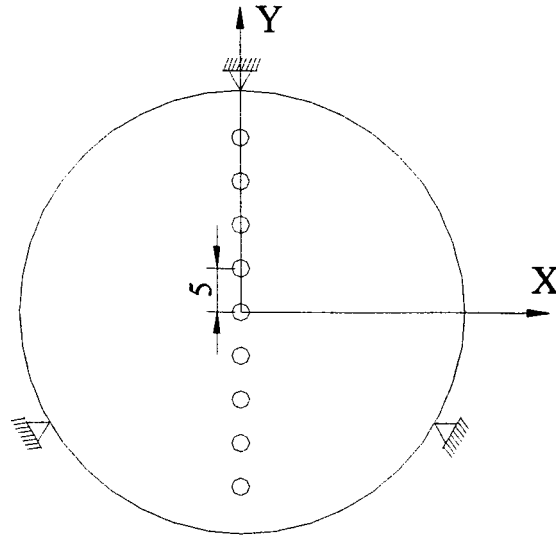


Figure 2. Distribution of excitation points for computing the deformation of the mirror

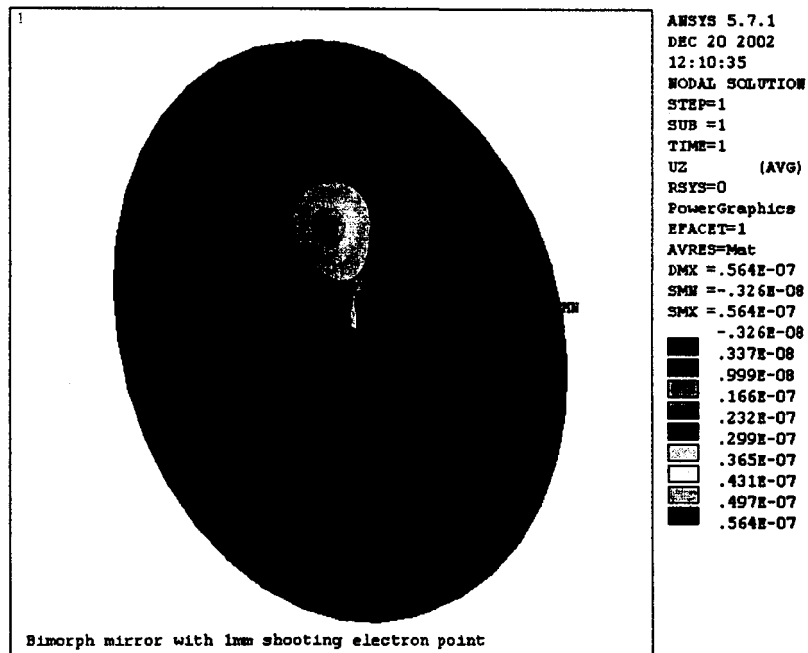


Figure 3. The deformation of the bimorph mirror actuating an electron point at (0,10) with 100 V

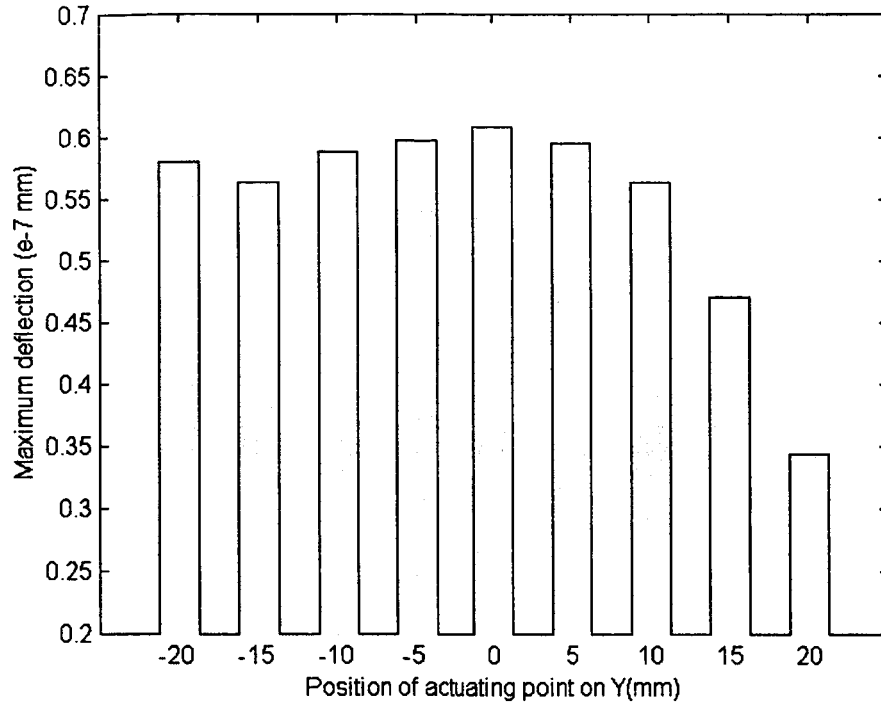


Figure 4. Maximum deflections on the mirror actuated at different positions with the same voltage

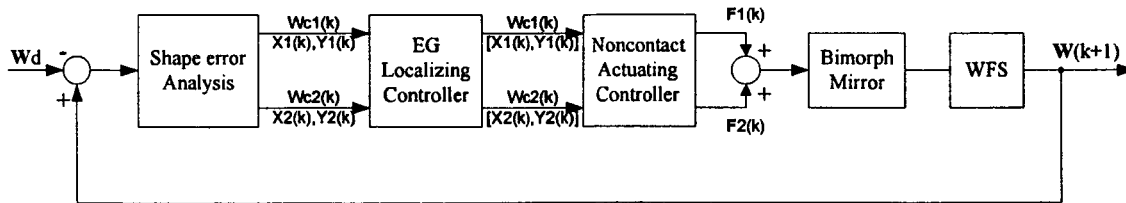


Figure 5. Block diagram of the feedback control system

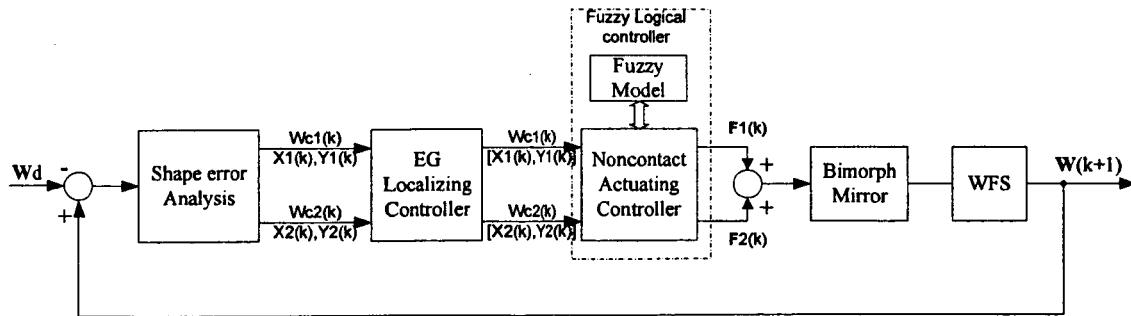


Figure 6. Block diagram of the fuzzy control system

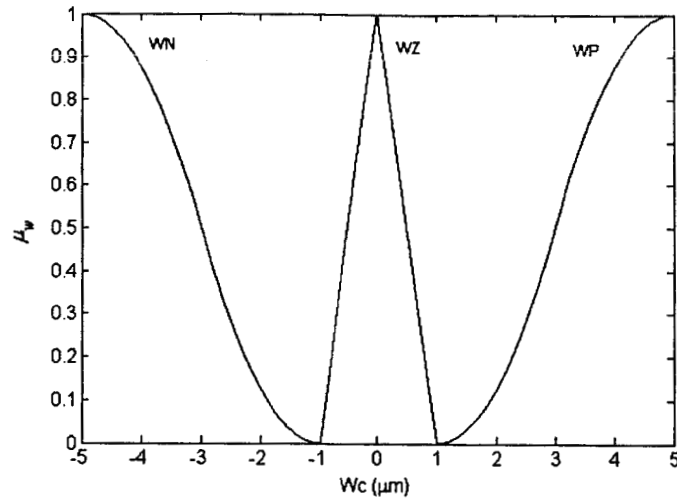


Figure 7. Membership function representation of deflection input

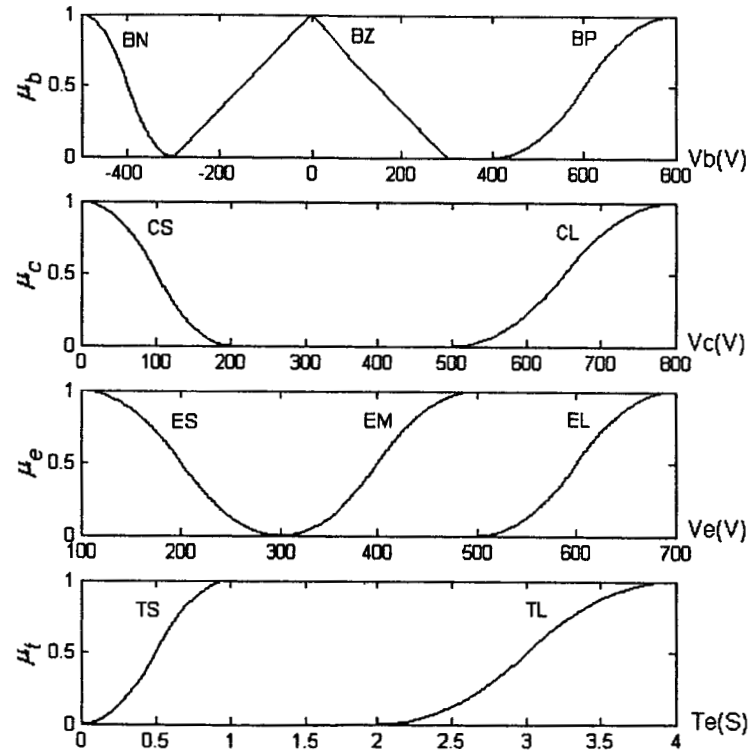


Figure 8. Membership function representation of output variables

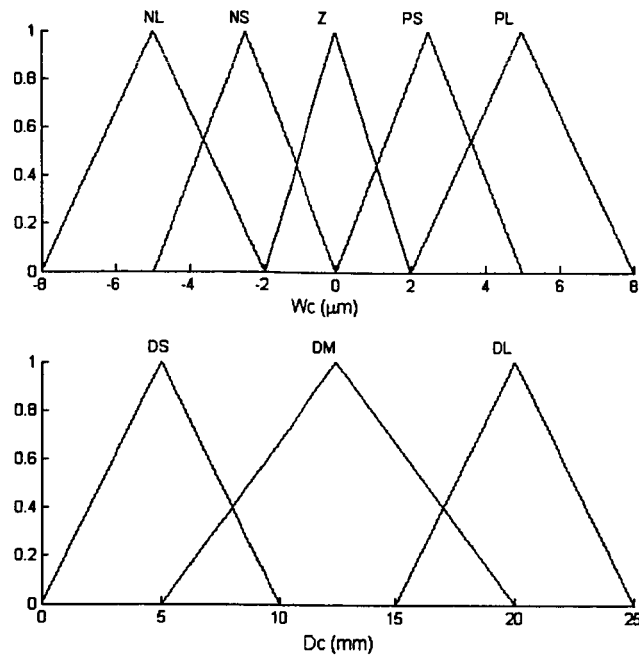


Figure 9. Membership function representations of input variables

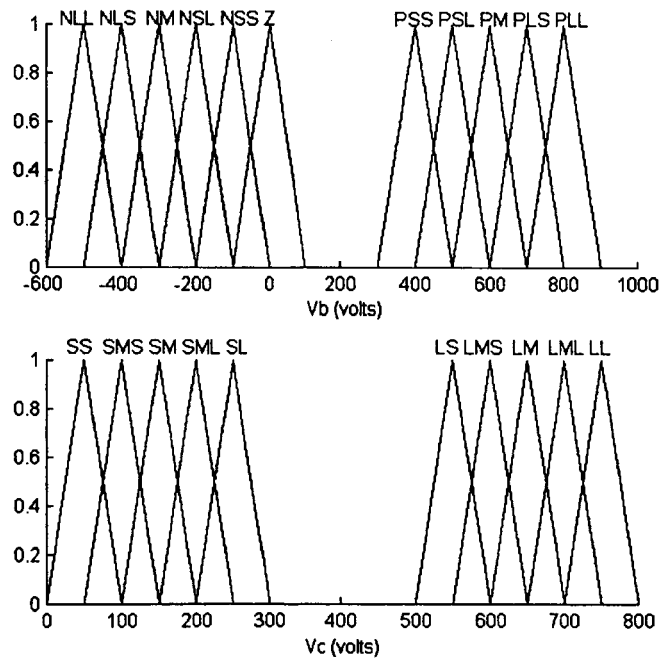


Figure 10. Membership function representations of  $V_b$  and  $V_c$

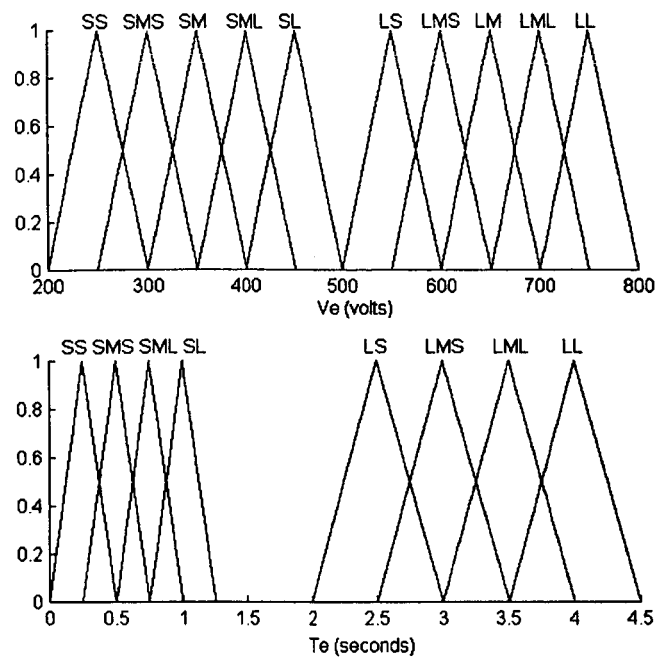
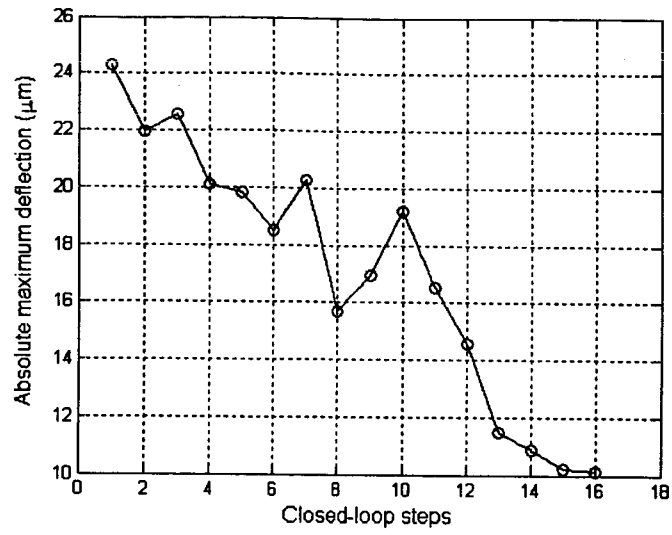
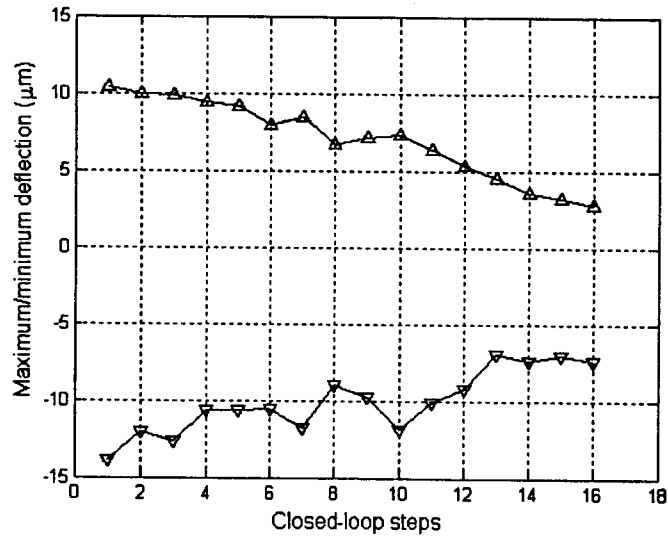


Figure 11. Membership function representations of  $V_e$  and  $T_e$

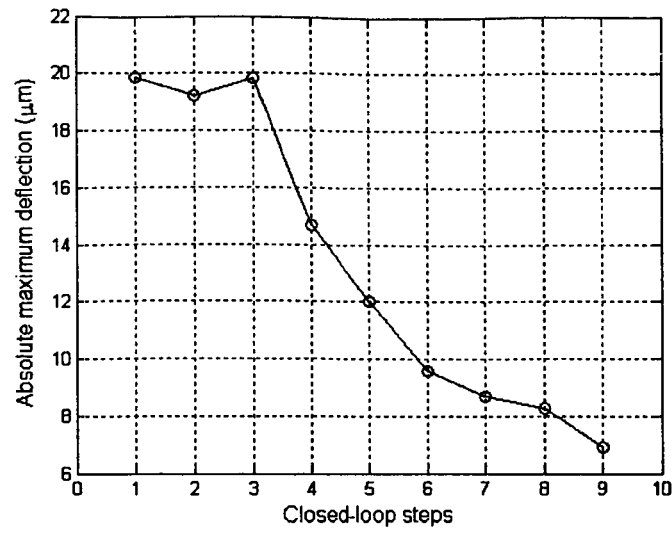


(a)

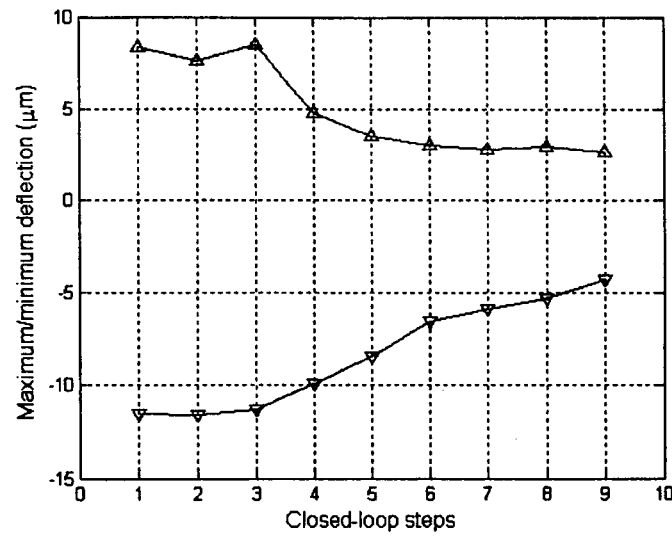


(b)

Figure 12. The deflection response using the SIMO fuzzy controller  
(a) Absolute maximum deflection (b) Max/min deflection

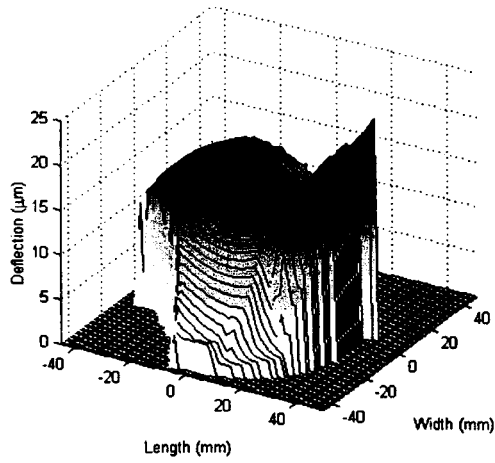


(a)

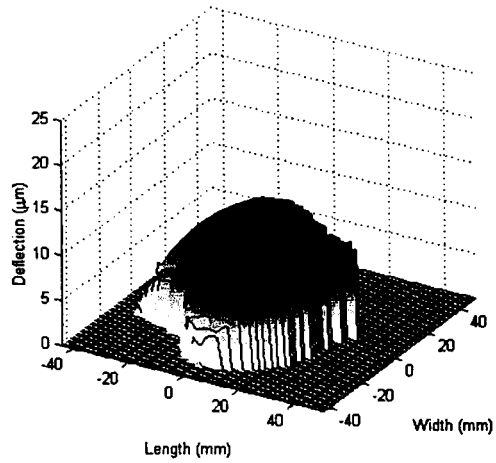


(b)

Figure 13. The deflection response using the MIMO fuzzy controller  
 (a) Absolute maximum deflection (b) Max/min deflection

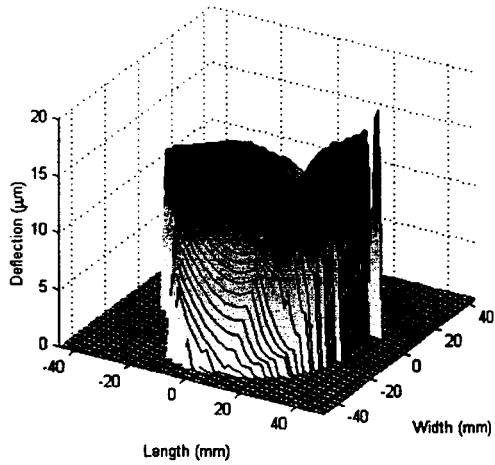


(a)

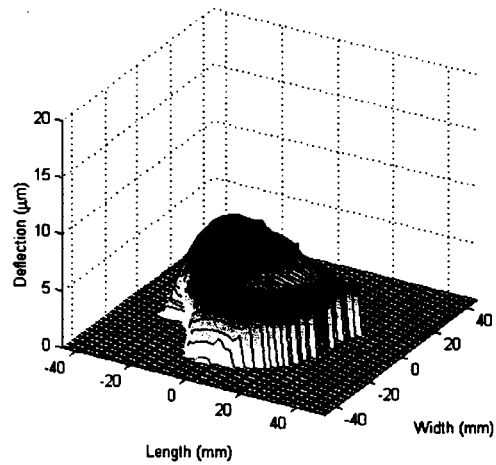


(b)

Figure 14. The initial and controlled profiles of the mirror with the SIMO fuzzy controller



(a)



(b)

Figure 15. The initial and controlled profiles of the mirror with the MIMO fuzzy controller